PHYSICAL REVIEW E VOLUME 60, NUMBER 2 AUGUST 1999

Phase separation with multiple length scales in polymer mixtures induced by autocatalytic reactions

Qui Tran-Cong,* Junji Kawai, Yukihiro Nishikawa,† and Hiroshi Jinnai
Department of Polymer Science and Engineering, Kyoto Institute of Technology, Matsugasaki, Kyoto 606-8585, Japan
(Received 16 February 1999; revised manuscript received 27 April 1999)

A ternary polymer blend with two components photo-cross-linked independently in its miscible region undergoes phase separation, exhibiting morphology with multiple length scales. Contrary to the case of thermally induced phase separation, the morphology exhibits a *unimodal→multimodal* transition. It is shown that these multiple length scales are caused by the inhomogeneous freezing kinetics of the cross-linking process. This inhomogeneity arises from the autocatalytic feedback driven by the couplings between concentration fluctuations and the photo-cross-linking reactions. [S1063-651X(99)50308-5]

PACS number(s): 83.80.Es, 83.80.Jx, 82.35.+t, 64.75.+g

Recent analytical theories and numerical calculations predict that the concentration fluctuations with long wavelengths, the so-called soft modes, in binary mixtures can be stabilized by chemical reactions [1–6]. This prediction was confirmed by experiments using binary polymer mixtures with one component undergoing reversible photoisomerization [7,8]. Similar suppression processes of these long wavelength fluctuations were also observed in experiments using photo-cross-linking reactions to freeze the polymer mobilities inside the spinodal [9] and the one-phase regions [10]. The resulting structures, known as modulated phases, have been observed over a wide range of experiments as well as by computer simulations in condensed matter [11,12]. The above-mentioned results suggest that chemical reactions can be used as a useful tool to manipulate the concentration fluctuations via which the morphology of polymer mixtures can be efficiently controlled.

In this Rapid Communication, we show that the morphology of a ternary polymer mixture can undergo a *unimodal →multimodal* transition induced by independent cross-linking reactions of its two polymer components. By simultaneously monitoring the reaction kinetics and the time evolution of the morphology, it was found that the multiple length scales arise from the inhomogeneity of the cross-linking process. The autocatalytic behavior of the reaction is responsible for this inhomogeneous kinetics, leading to the emergence of the morphologies with multiple length scales.

Samples used in this work are tertiary mixtures of anthracene (*A*)–labeled polystyrene (PSA, $M_w=2.2\times10^5$, $M_w/M_n=1.7$), polystyrene labeled with a cinnamic acid derivative (*C*) (PSC, $M_w=2.2\times10^5$, $M_w/M_n=1.7$) and poly(vinyl methyl ether) (PVME, $M_w=1.0\times10^5$, $M_w/M_n=2.5$). Except for PVME, which was purchased from Aldrich, the other two polymers were synthesized according to the method reported previously [8,9]. The sample thickness was fixed at 50 μm by using a spacer. Other characteristics, such as sample sizes and the preparation procedure of the blends, were described in detail elsewhere [10].

The cloud points of PSA/PSC/PVME ternary blends were measured by light scattering at a fixed angle (20°) with a heating rate of 0.2 °C/min. By varying the weight fraction (ϕ) of the blend so that $\phi_{PSA}=\phi_{PSC}$, while ($\phi_{PSA}+\phi_{PSC}$) is varied, it was found that these blends exhibit a lower critical solution temperature located at ($\phi_{PSC}+\phi_{PSA}$)$\cong$20% wt. All of the blends reported throughout this paper have the composition PSA/PSC/PVME (20/20/60 %). Morphology was observed by using a phase-contrast optical microscope (Nikon, model FTX-21) and was digitized using an image analyzer (Pias, LA-525, Japan). Further analysis of these images was performed on a Macintosh computer (model 7100/80AV) by two-dimensional fast Fourier transform (2D-FFT) using standard softwares for image analysis (Scion Image [13] and Super Paint). The characteristic length scale ξ of the morphology was calculated by using the Bragg relation $\xi=2\pi/q_{max}$. Here, q_{max}, the wave number corresponding to the maximal intensity obtained from the 2D-FFT of the images, was calculated by circular averaging the two-dimensional intensity distribution $I(q)$:

$$I(q)=F(\mathbf{q})\cdot F(\mathbf{q})^*. \tag{1}$$

The structure amplitude $F(\mathbf{q})$ in the above equation is the Fourier transform of the contrast $\{C(\mathbf{r})-C_0\}$ of the optical micrograph defined by

$$F(\mathbf{q})=\int_{-\infty}^{\infty}\{C(\mathbf{r})-C_0\}e^{-i\mathbf{q}\cdot\mathbf{r}}d\mathbf{r}, \tag{2}$$

where C_0 is the average concentration of the image and $F(\mathbf{q})^*$ is the complex conjugate of $F(\mathbf{q})$.

A Hg-Xe lamp (Hamamatsu Photonics, 500 W) was used as a light source to induce cross-linking reactions of PSA and PSC chains via photodimerization of anthracene (*A*) and of *trans-cinnamic* acid derivative (*C*) [14]. Ultraviolet (uv) light with wavelengths longer than 360 nm and 280 nm was used respectively to induce the only *A-A* (*single cross-link*) and the *A-A*, *C-C* simultaneous (*double*) cross-linking reactions. The light intensity at 365 nm was adjusted at 3.0

*Author to whom correspondence should be addressed. Electronic address: qui@ipc.kit.ac.jp

†Present address: Department of Polymer Chemistry, Kyoto University, Sakyo-ku, Kyoto 606, Japan.

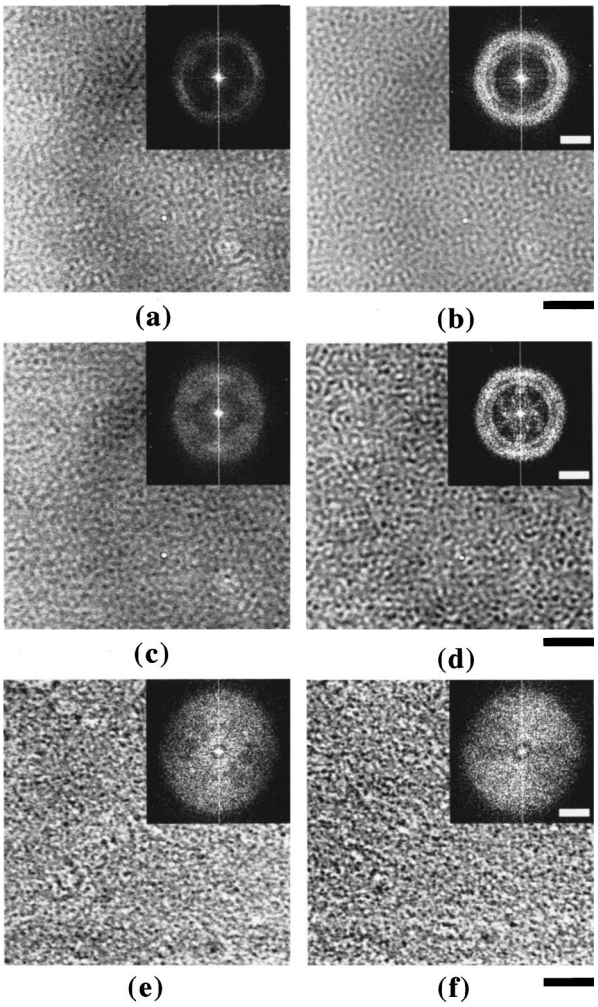

FIG. 1. Morphology and the corresponding 2D-FFT intensity distribution of a PSA/PSC/PVME (20/20/60 %) blend. An *A-A*, *C-C double* photo-cross-link at 110 °C in 60 min (a) and 80 min (b); *only* the *A-A* photo-cross-link at 110 °C in 110 min (c) and 250 min (d); *A-A*, *C-C* double photo-cross-linked at 40 °C for 30 min and then jumped to 145 °C in the dark, annealing time: 30 min (e) and 50 min (f). The scales are respectively 2×10^4 cm^{-1} and 10 μm for the Fourier intensity distribution and the images.

mW/cm^2. The inhomogeneity of the light intensity within the area covering the sample size ($12\times6\times0.05$ mm) is not more than $\pm5\%$.

At first, PSA and PSC chains in a PSA/PSC/PVME (20/20/60 %) blend were simultaneously photo-cross-linked at 110 °C, which is 40 °C below the phase boundary. The regular cocontinuous morphology becomes observable at 25 min of irradiation. As an example, the morphology obtained after 60 min of irradiation and its 2D-FFT intensity distribution as a ''sharp ring'' are shown in Fig. 1(a). As irradiation time increases, the morphology coarsens very slowly and, subsequently, the second ring appears at the inner (low wave number) side of the preexisting ring as depicted in Fig. 1b for the same blend irradiated over 80 min. In order to confirm the existence of multiple length scales in the phase separation of the PSA/PSC/PVME blend induced by the double cross-link reactions, inverse Fourier transform of the structure amplitude $F(\mathbf{q})$ given in Eq. (2) was performed by separately masking the low q range ($q<3.0\times10^4$ cm^{-1}) and the high q range ($q>3.0\times10^4$ cm^{-1}) of the 2D-FFT intensity distribution shown in the inset of Fig. 1(b). The value $q=3.0\times10^4$ cm^{-1} corresponds to the magnitude of q located between the two rings of the intensity distribution. As illustrated in Fig. 2, two distinct morphologies with different length scales were resolved from the inverse 2D-FFT operation. Furthermore, the original morphology illustrated in Fig. 1(b) was recovered by superimposing the two morphologies resolved in Figs. 2(b) and 2(c). It is worth noting that the intensity distribution similar to those in the inset of Fig. 1(b) was also observed by 2D light scattering under the same condition. However, we only used the data obtained by optical microscopy for further analysis because the scattering patterns observed with light scattering are often distorted by the inhomogeneity arising from the cross-linking reactions of the blend. Furthermore, since the morphology of the cross section of the irradiated blends is uniform within the irradiation time of these experiments, the contribution of the light intensity gradient inside the sample can be ruled out under these experimental conditions.

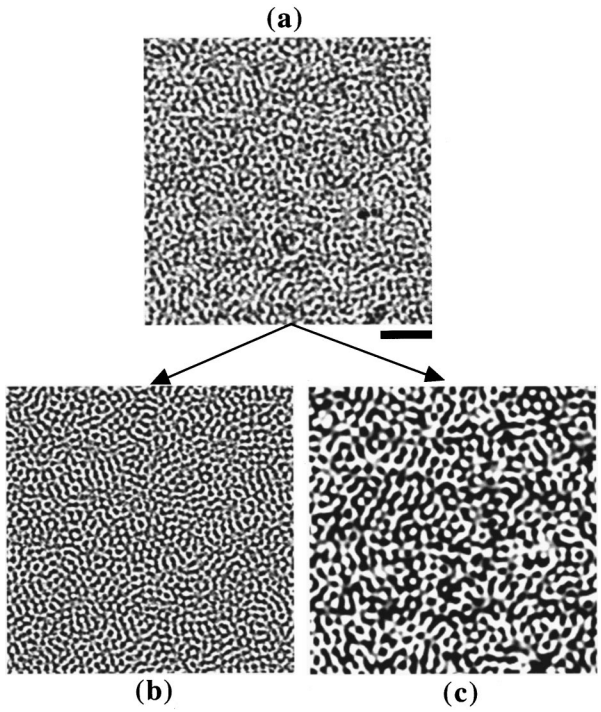

FIG. 2. Morphology with multiple characteristic length scales resolved by inverse FFT: (a) original morphology obtained by *A-A*, *C-C double* cross-links of a PSA/PSC/PVME (20/20/60 %) blend after 80 min of irradiation at 110 °C; (b) cocontinuous morphology with $q>3.0\times10^4$ cm^{-1}; (c) cocontinuous morphology with $q<3.0\times10^4$ cm^{-1}.

Unlike the case of *double* cross-links, phase separation of the same blend induced by *only* the *A-A* cross-link under the same condition began with a ''broad ring.'' An example is illustrated in Fig. 1(c) for a PSA/PSC/PVME (20/20/60 %) blend irradiated with 365 nm uv light for 110 min at 110 °C. As irradiation time increases, though the characteristic length scale of the morphology is almost time independent, their contrast is getting stronger and the intensity $I(\mathbf{q})$ with broad distribution obtained by 2D-FFT splits into two distinct rings shown in Fig. 1(d), as an example, for a blend irradiated over

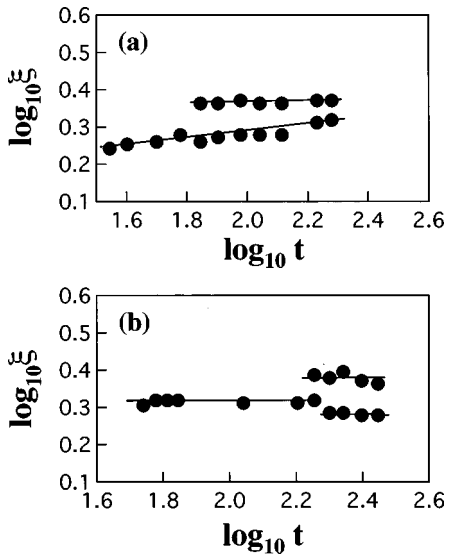

FIG. 3. Time evolution of the characteristic length scales obtained for a PSA/PSC/PVME (20/20/60 %) blend photo-cross-linked at 110 °C: (a) *A-A* and *C-C* simultaneous cross-links; (b) only the *A-A* cross-link.

250 min. In order to elucidate the role of the chemical reactions playing in the phase separation with multiple length scales, a PSA/PSC/PVME blend was slightly cross-linked by irradiating the blend for 30 min at 40 °C. At this stage, the blend remains miscible with a cross-link density (γ) of two junctions/chain for PSA chains and an almost negligible amounts of the *C-C* cross-links for the PSC component. Subsequently, the light source was turned off and the cross-linked blend was jumped from 40 °C to 145 °C in the dark with a jump depth of 5 °C. The phase separation was then promoted by annealing the reacted blend at this destination temperature. Contrary to the case shown in Figs. 1(a)–1(d), no spinodal rings were observed while the 2D-FFT intensity increased with annealing time. These results clearly indicate that the *in situ* cross-linking reactions play a crucial role in the emergence of multiple length scales in the phase separation of PSA/PSC/PVME blends.

Shown in Fig. 3 is the time evolution of the characteristic length scale ξ obtained from the 2D-FFT intensity $I(\mathbf{q})$ of a PSA/PSC/PVME (20/20/60 %) blend with the *A-A* and *C-C* *double* cross-linking reactions [Fig. 3(a)], and the *A-A* *single* cross-linking reaction [Fig. 3(b)]. In the former case, the time evolution of the structure proceeds slowly under irradiation and can be expressed by the power law $\xi \propto t^{\alpha}$ with $\alpha \cong 0.1$. However, at ca. 70 min after irradiation, an inner ''ring'' appears. Its characteristic length scale is almost independent from the irradiation time ($\alpha = 0.02$) and tends to merge into the ''outer ring'' at long irradiation time. Compared to this *double* cross-linking reaction, phase separation of the same blend with *only* the *A-A* cross-links, performed under the same experimental conditions, proceeds differently as seen in Fig. 3(b). The characteristic length scale ξ estimated from the broad 2D-FFT intensity of Fig. 1(c) stays almost constant over the first 160 min of irradiation. However, beyond this range of irradiation time, ξ becomes multiple [see Fig. 1(d)]. These two length scales remain unchanged within 120 min of additional irradiation.

In order to correlate the cross-linking processes and the resulting morphology, the reaction kinetics was directly monitored by following the changes in optical densities of anthracene on the PSA chains at 400 nm, and of cinnamic acid ester groups on the PSC chains at 310 nm prior to phase separation. The conversion $\alpha(t)$ of these reactions at a time t was calculated by using the definition $\alpha(t) = [OD(t=0) - OD(t)]/OD(t=0)$, where $OD(t=0)$ and $OD(t)$ are, respectively, the absorbances of anthracene and cinnamic acid moieties measured before and after t min of irradiation. As shown in Fig. 4, the mean reaction rate given by $(d\alpha/dt)$ for the photodimerization of cinnamic acid decreases quickly with irradiation time and almost vanishes at 20 min after irradiation at 110 °C. The corresponding total conversion was 4% (equivalent to one *C-C* junction/chain) over this period of irradiation prior to phase separation. These data indicate that the *C-C* cross-linking reaction did not proceed efficiently under these experimental conditions. On the other hand, the photodimerization of anthracene on the PSA chains is more efficient with a total yield of 31.3% (equivalent to six *A-A* junctions/chain) and 23.8% (five *A-A* junctions/chain) for the cases of *only* *A-A* and *A-A*, *C-C* *double* cross-links, respectively, during the same period of irradiation. The difference in the cross-link density obtained for these two cases is consistent with the different coarsening kinetics illustrated in Fig. 3. As depicted in Fig. 4, the irradiation-time dependence of the average reaction rate $d\alpha(t)/dt$ of anthracene exhibits a maximum at the early stage of the reaction (ca. 4 min after irradiation) and gradually decreases with increasing irradiation time. These results are in strong contrast with the $d\alpha(t)/dt$ data of cinnamic acid, revealing the autocatalytic behavior of the *A-A* cross-linking reactions under irradiation. Such autocatalytic behavior of the *A-A* cross-linking reaction has been observed previously in the photo-cross-linking kinetics of binary polymer blends and was attributed to the couplings between the cross-linking reactions and the concentration fluctuations of the reacting blend [15]. The position of the maximum of $d\alpha(t)/dt$ in Fig. 4 is determined by the competition between the acceleration of the reaction by irradiation and the deceleration caused by the increase in viscosity of the environments around the PSA chains. Shown in the same figure is the reaction kinetics of *only* the *A-A* cross-links selectively induced among the PSA chains in the same ternary blend.

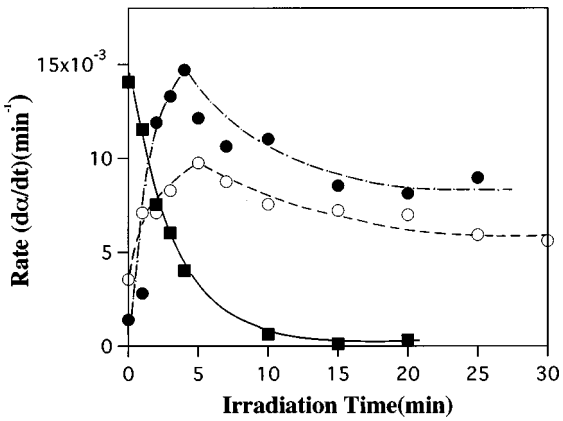

FIG. 4. Irradiation time dependence of the average reaction rates obtained at 110 °C: ●, *A-A* and *C-C* simultaneous cross-links; ○, only the *A-A* cross-link; ■, only the *C-C* cross-link.

Obviously, the reaction also exhibits the autocatalytic behavior with a maximum in $d\alpha(t)/dt$ at ca. 4 min of irradiation. These results suggest that the cross-linking reaction of PSC chains performed via photodimerization of cinnamic acid did not actively participate in the phase separation.

It should be noted that the phase separation with multiple characteristic length scales observed in this work shares a common feature with the phase separation kinetics of polymer blends with hydrogen bonding reported previously by using *T*-jump light scattering [16] and more recently in a study of hydrogen bonding distribution in miscible polymer blends by using small-angle neutron scattering [17]. Furthermore, the morphology with bimodal droplets has been experimentally found in thermal curing of epoxies [18] and more recently in a computer simulation of polymerization-induced phase separation where the polymer mobilities are gradually slowed down with an increase in the reaction conversion [19]. From the above results, we conclude that the inhomogenous reaction kinetics enhanced by the presence of some autocatalytic mechanism is responsible for the emergence of these multiple length scales in the phase separation of polymer mixtures. Since all of the blends used in this study are miscible at the experimental temperatures and can only undergo phase separation when the reactions proceed, it is reasonable to think that the two length scales appearing in Fig. 1 likely come from the phase separation of PVME and cross-linked species with various distribution. In order to quantitatively explain the complex kinetics of the phase separation described above, some theoretical models incorporating the autocatalysis of the reactions into the equation of motion, such as the time-dependent Ginzburg-Landau equation for polymer mixtures, are currently in need.

This work was financially supported by the Ministry of Education, Culture and Science, Japan (Grant No. 09650998).

[1] B. A. Huberman, J. Chem. Phys. **65**, 2013 (1976).
[2] S. C. Glotzer, E. A. Di Marzio, and M. Muthukumar, Phys. Rev. Lett. **74**, 2034 (1995).
[3] J. Verdasca, P. Borckmans, and G. Dewel, Phys. Rev. E **52**, 4616 (1995); **55**, 4828 (1997).
[4] J. J. Christensen, K. Elder, and H. C. Fogedby, Phys. Rev. E **54**, 2212 (1996).
[5] D. Carati and R. Lefever, Phys. Rev. E **56**, 3127 (1997).
[6] M. Hildebrand, A. S. Michailov, and G. Ertl, Phys. Rev. E **58**, 5483 (1998).
[7] Q. Tran-Cong, T. Ohta, and O. Urakawa, Phys. Rev. E **56**, R59 (1997).
[8] T. Ohta, O. Urakawa, and Q. Tran-Cong, Macromolecules **31**, 6845 (1998).
[9] A. Imagawa and Q. Tran-Cong, Macromolecules **28**, 8388 (1995).
[10] A. Harada and Q. Tran-Cong, Macromolecules **30**, 1643 (1997).
[11] M. Seul and D. Andelman, Science **267**, 476 (1995).
[12] C. Sagui and R. C. Desai, Phys. Rev. E **49**, 2225 (1994).
[13] Scion Image for MAC OS is an extended version of the NIH Image Program (developed at the U.S. National Institutes of Health) available on the Internet at URL: http://scioncorp.com/pages/scion_image_mac.html.
[14] See, for example, J. J. McCullough, Chem. Rev. **87**, 811 (1987).
[15] Q. Tran-Cong, A. Harada, K. Kataoka, T. Ohta, and O. Urakawa, Phys. Rev. E **55**, R6340 (1997).
[16] M. He, Y. Liu, Y. Feng, M. Jiang, and C. C. Han, Macromolecules **24**, 464 (1991).
[17] C. Zhou, E. K. Hobbie, B. J. Bauer, and C. C. Han, J. Polym. Sci., Part B: Polym. Phys. **36**, 2745 (1998).
[18] T. Ohnaga, J. Maruta, and T. Inoue, Polymer **30**, 1845 (1989).
[19] M. Okada, H. Masugawa, and H. Furukawa (unpublished).